JOURNAL OF Applied Polymer SCIENCE

The Influence of Melt-Mixing Process Conditions on Electrical Conductivity of Polypropylene/Multiwall Carbon Nanotubes Composites

Pankaj B. Tambe,* Arup R. Bhattacharyya, Ajit R. Kulkarni
Department of Metallurgical Engineering and Materials Science, Indian Institute of Technology Bombay, Powai, Mumbai, India
*Present address: School of Mechanical and Building Sciences, VIT University, Vellore 632014, India

Correspondence to: A. R. Bhattacharyya (E-mail: arupranjan@iitb.ac.in)

ABSTRACT: The influence of melt-mixing parameters on the development of "network-like" structure of multiwall carbon nanotubes (MWNTs) in injection-molded polypropylene (PP)/MWNTs composites was assessed through AC electrical conductivity measurements. A higher melt-mixing temperature (260°C as compared to 200, 220, and 240°C) at a fixed rotational speed of the screws (150 rpm) and at a fixed mixing time (15 min) has yielded maximum improvement in electrical conductivity in PP/MWNTs composites of 3 wt % MWNTs content. Next to higher melt-mixing temperature, a variation in the melt-mixing time has also led to a variation in electrical conductivity of the composites. Raman spectroscopic analysis revealed an increase in the ratio of intensity due to *G*-band over that of *D*-band (I_G/I_D) of the MWNTs in the "skin" region as compared to the "core" region of the injection-molded composites irrespective of the melt-mixing conditions. Microscopic observations could not provide much insight into the variation of MWNTs network-like structure in various PP/MWNTs composites. An attempt has been made to understand the variation of network-like structure of MWNTs in PP/MWNTs composites as a function of melt-mixing parameters through electrical conductivity measurements, Raman spectroscopic analysis, and morphological investigations. © 2012 Wiley Periodicals, Inc. J. Appl. Polym. Sci. 000: 000–000, 2012

KEYWORDS: polypropylene; multiwalled carbon nanotubes; dispersion; melt mixing

Received 19 May 2010; accepted 16 April 2012; published online
DOI: 10.1002/app.37889

INTRODUCTION

Polypropylene (PP) is one of the important commodity plastics in view of its consumption in commodity applications. However, PP can be suitably modified to improve its performance for engineering applications. It has been reported that polymer/carbon nanotubes (CNTs) composites exhibit high strength and stiffness along with high electrical conductivity at relatively low concentration of CNTs.[1,2] The high aspect ratio of CNTs makes it enable to form percolating "network-like" structure (electrical percolation) at relatively low CNTs content.[3,4] Theoretical analysis using numerical method has been used to predict the electrical and thermal conductivity of functionally graded materials/composites.[5,6]

However, uniform dispersion of CNTs in a polymer matrix has been posed to be a difficult task due to the "agglomeration" of CNTs along with their "entangled" network. It has also been reported that breakdown of CNTs "cluster" or "aggregates" into individual CNT is necessary to achieve lower electrical percolation threshold in the polymer matrix.[7] Besides promoting shearing action during melt mixing,[8] organic modifier has also been reported to reduce the CNTs aggregate size, which has resulted in low electrical percolation threshold in various polymer composites involving multiwall carbon nanotubes (MWNTs).[9–12]

The state of dispersion of CNTs in the respective polymer composites has been investigated through electrical conductivity measurements along with microscopic characterization.[7,8] Moreover, injection-molded polymer/CNTs composites at a fixed CNTs concentration exhibit higher electrical percolation threshold as compared to corresponding compression-molded sample due to the orientation of CNTs in the "skin" region in the injection-molded specimen, which leads to a difficulty in forming random network-like structure in three dimension (3D) involving skin as well as "core" region of the specimen.[13,14]

The network-like structure formation of CNTs in the melt state has been affected in polymer/CNTs composites prepared through melt mixing during solidification, which has been studied through electrical conductivity measurements. The electrical conductivity measurements during melt state indicated a very low electrical percolation threshold ($0.0025 < \phi < 0.01$) in MWNTs-filled PP composites[15]; however, the room temperature

conductivity measurement of PP/MWNTs showed a higher electrical percolation threshold.[16] Further, Alig et al.[17] conducted *in situ* electrical conductivity measurements on PP/MWNTs composites wherein it has been found that electrical conductivity at solid state was significantly lower than the melt state due to a reduction of the amorphous phase at the expense of the crystalline phase.

Various studies have been conducted in recent times on melt-mixed PP/CNTs composites that were primarily focused on the various parameters influencing the state of CNTs dispersion.[18–22] PP/MWNTs composites prepared via masterbatch dilution process showed a higher electrical percolation threshold in the presence of PP-g-MA; however, lower molar mass PP chains lead to a lower electrical percolation threshold due to a better infiltration/adsorption of shorter PP chains during masterbatch dilution.[18] The state of dispersion of MWNTs has also been assessed in the PP matrix using electrical conductivity measurements along with nonisothermal crystallization studies of the PP phase.[19] A low electrical percolation threshold ($\sim$ 0.6 vol % of MWNTs) has been observed in melt-mixed PP/MWNTs composites in which the composites were processed through masterbatch dilution approach.[20] Raman mapping along with rheological studies and crystallization kinetics was used to investigate the state of dispersion of SWNTs in PP/SWNTs composites.[21] The influence of PP-g-MA on the state of MWNTs dispersion has also been evaluated through rheological studies in melt-mixed PP/MWNTs composites.[22] Influence of various types of MWNTs on the electrical conductivity and the state of dispersion of MWNTs in PA12 matrix was studied in melt-mixed PA12/MWNTs composites.[23]

Even though a large body of literatures exist on melt-mixed polymer/CNTs composites in general and on PP/CNTs composites in specific dealing with the state of dispersion of CNTs and the corresponding properties (*viz.*, electrical conductivity and mechanical/dynamic mechanical properties) of the composites, very few literatures are available on the influence of melt-mixing parameters on the state of CNTs dispersion in PP matrix. Krause et al.[8] found that higher mixing temperature at low rotational speed for higher mixing time was found to be the best optimized condition during melt mixing in a DACA microcompounder for dispersion of MWNTs in polyamide matrix. A specific set of melt-mixing protocol has resulted in lower electrical percolation threshold (1 wt %) of MWNTs in polyamide 66 matrix. Villmow et al.[24] found that higher rotational speed (500 rpm) and a fixed residence time of the melt combined with a specific screw profile significantly influenced the dispersion of MWNTs in polylactic acid matrix during masterbatch and dilution step in a twin-screw extruder. However, these results are often based on matrix-specific [*viz.*, PA and polycarbonate (PC)-based MWNTs composites] observation and cannot be extended to all the polymer matrices in general. Keeping in view of the above, the influence of melt-mixing parameters on the electrical conductivity was investigated in injection-molded PP/MWNTs composites at a fixed concentration of 3 wt % of MWNTs. This specific composition has been selected based on our earlier result that shows that this composition (PP + 3 wt % MWNTs) exhibits far above the electrical percolation threshold of MWNTs[12] in PP/MWNTs composites. An attempt has been made to understand the role of melt-mixing parameters on the electrical conductivity of the PP/MWNTs composites. Simultaneously, the composites were characterized through morphological observation by scanning electron microscopic (SEM) analysis and transmission electron microscopic (TEM) analysis. Moreover, Raman spectroscopic analysis has been used for evaluating MWNTs network-like structure in the skin as well as in the core of PP/MWNTs composites.

EXPERIMENTAL

Materials and Composite Preparation

PP was obtained from Reliance Industries, India (REPOL H200FG, melt flow index of 20 g/10 min at 230°C with a load of 2.16 kg. Purified MWNTs were procured from Nanocyl CA, Belgium (NC 3100, purity >95%, diameter: 9.5 nm, average length 1.5 μm; as per manufacturer's specifications). PP/MMWNTs composites were prepared by melt mixing in a conical twin screw microcompounder (Micro 5; DSM Research, The Netherlands, which is a batch mixer) as a function of MWNTs concentration. MWNTs concentration has been varied from 0.5 to 5 wt % at 240°C, 150 rpm for 10 min. Compression-molded films of 0.5-mm thickness were used for electrical conductivity measurements. A detailed discussion on these composites can be found in Ref. [12]. PP/MWNTs composites of 3 wt % MWNTs were also prepared by melt mixing in a conical twin-screw microcompounder by varying melt-mixing parameters (screw speed, mixing time, and mixing temperature). The actual melt temperature for the various mixing protocols was found to be well within the set temperature of melt mixing. The melt-mixing parameters along with sample codes are provided in Table I. Injection-molded samples (ASTM D 638, Type V) were prepared using mini injection molding machine from DSM Research (Netherlands). The injection molding parameters maintained for all the compositions were injection pressure 3 bar, melt temperature 260°C, mold temperature 60°C, holding time 2 min, and cooling time 2–3 min.

Characterization

AC electrical conductivity measurements were performed using compression-molded and injection-molded (across the thickness) samples in the frequency range between 10^{-1} and 10^{6} Hz using Novocontrol Alpha high-resolution analyzer. The samples were placed in between the gold electrodes. DC electrical conductivity of the sample was determined from the frequency-independent AC electrical conductivity plateau by fitting power law equation ($\sigma_{AC} = \sigma_{DC} + A\omega^n$; $0 < n < 1$, where σ_{AC} = AC electrical conductivity, σ_{DC} = DC electrical conductivity, ω = frequency, "A" is a constant dependent on temperature, and "n" is an exponent dependent both on temperature and frequency).[25]

SEM analysis was performed with Hitachi S3400, operated at 15 kV with gold sputtering on the cryofractured surfaces of the extruded strands of the composite samples. For TEM analysis, core of the injection-molded sample was used. Injection-molded samples were microtomed to obtain ultrathin sections at room temperature using Leica Ultramicrotome Microsystems. Samples were collected on a TEM grid. TEM investigation was performed with Philips CM 200 instrument at 200 kV.

Table I. Various Processing Parameters During Melt Mixing of PP/MWNTs Composites of 3 wt % MWNTs

Sr. no.	Sample code	Temperature (°)	Screw speed (rpm)	Time (min)	Mixing energy (J/cm^3)
1	T-260	260	150	15	5491.8
2	T-240	240	150	15	7340.1
3	T-220	220	150	15	8285.8
4	T-200	220	150	15	8886.8
5	R-50	260	50	15	832.7
6	R-100	260	100	15	2983.4
7	R-200	260	200	15	8440.3
8	Ti-5	260	150	5	2575.4
9	Ti-10	260	150	10	4216.3
10	Ti-20	260	150	20	7471.9

Raman spectroscopy was performed using Jobin Yovon (HR 800 micro-Raman) in the scanning range of 200–2000 cm^{-1} with incident laser excitation wavelength of 514 nm using injection-molded specimen of the skin and the core region.

RESULTS AND DISCUSSION

Torque During Melt Mixing

It is observed that torque value during melt mixing of PP and MWNTs provides an indirect observation of the melt viscosity of the composites. The variation of torque as a function of varying melt-mixing parameters for PP/MWNTs composites of 3 wt % MWNTs is presented in Figure 1. Figure 1(a) shows that torque value decreases with increase in melt-mixing temperature at a fixed set of mixing time (15 min) and rotational speed (150 rpm) of the screws. In general, torque is found to be higher in the initial mixing time due to incomplete melting of PP and indicates an increase in melt viscosity. With increase in mixing time torque is found to be lower, which indicates a decrease in melt viscosity due to the shear induced unentanglement of the polymer chains. It is expected that the shear forces exerted on the melt during melt-mixing decreases with an increase in melt-mixing temperature as unentangling the polymer chains requires lower extent of shear forces at the higher mixing temperature, which perhaps leads to the better infiltration/adsorption of the PP chains in between the MWNTs aggregates. At this melt-mixing condition, it may be expected that the aggregates size of MWNTs would be lowered in PP/MWNTs composites.

The torque value increases gradually with an increase in screw speed at a fixed set of mixing time (15 min) and temperature (260°C) [Figure 1(b)]. As the shear forces experienced by the melt are expected to increase with an increase in rotational speed of the screw, torque value increases with increase in rotational speed of the screw. However, as expected, the torque value remains almost same with an increase in mixing time (figure not shown here). Further, electrical conductivity measurement (discussed in the next section) shows a variation in electrical conductivity in PP/MWNTs composites with increasing melt-mixing time, which may arise due to a variation in the network-like structure of MWNTs (due to MWNTs breakage), which is not manifested in the torque data. A careful observation of the torque data for PP/MWNTs composites reveals that torque data varied significantly as a function of melt-mixing temperature, which is otherwise related to the melt viscosity of PP phase. Furthermore, torque data may not be sensitive to MWNTs attrition for prolonged melt-mixing time.[26] At this point, it is difficult to comment whether MWNTs attrition has

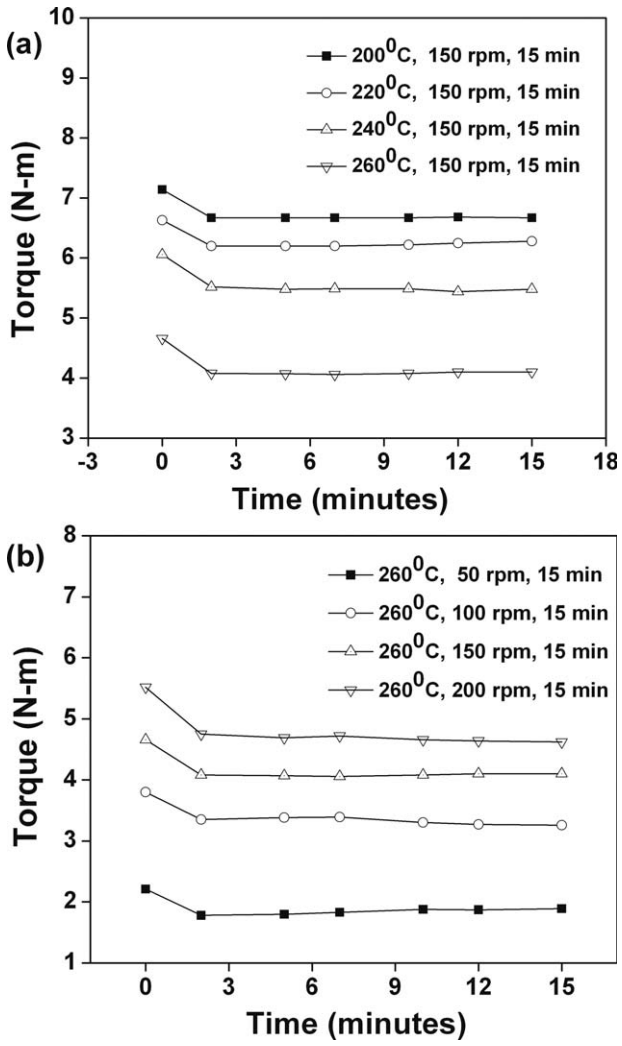

Figure 1. Variation of torque as a function of (a) mixing temperature and (b) screw speed during melt mixing of PP and MWNTs.

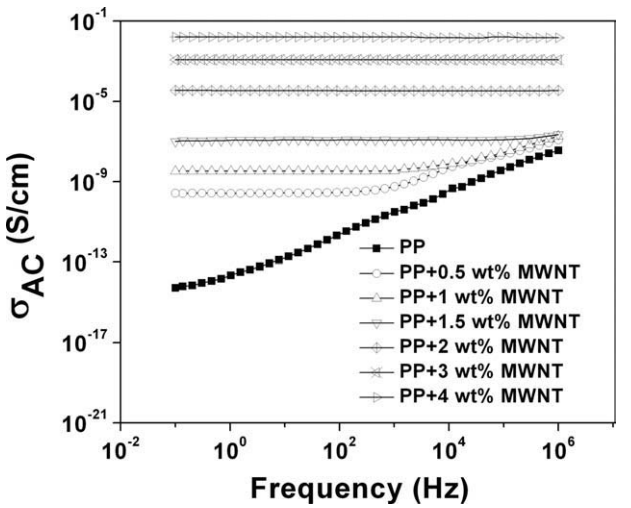

Figure 2. Variation of AC electrical conductivity as a function of frequency for compression-molded PP/MWNTs composites of varying MWNTs concentration.

been taken place during the initial stage of melt mixing or with prolonged melt-mixing time. A direct observation through TEM analysis would be effective to address this issue.

Krause et al.[8] explained the observed electrical conductivity data of PA6/MWNTs and PA66/MWNTs composites on the basis of "mixing energy" calculation together with macrodispersion index (a parameter based on the size of the remaining MWNTs aggregates through optical microscopy). In the present context, the mixing energy "E" during melt mixing was determined with the help of following equation[8]:

$$E = \int_0^t P dt = \int_0^t 2\pi \cdot N \cdot \tau dt,$$

where P is the engine output dependent on the time, τ is the torque that was measured during the mixing process, N is the rotational speed in revolution per minutes (rpm), and t is the mixing time. The torque value was calculated by multiplying the force value obtained during melt mixing with the average screw radius.

Mixing energy calculation as a function of melt-mixing parameters of PP/MWNTs composites was performed to understand whether the mixing energy calculation can provide any quantitative understanding for assessing the state of MWNTs dispersion. Table I exhibits the mixing energy as a function of melt-mixing parameters (screw speed, mixing time, and temperature). Mixing energy decreases with an increase in temperature, this manifests in a decrease in melt viscosity with an increase in mixing temperature from 200 to 260°C. However, mixing energy increases with an increase in screw speed from 50 to 200 rpm. Because of high shearing action, MWNTs aggregates may possibly break into smaller aggregates in a viscous PP.[17] Mixing energy increases by more than 3 orders of magnitude, while increasing the screw speed from 50 to 100 rpm, whereas it increases about 2 orders of magnitude from 100 to 150 rpm, whereas at 200 rpm, mixing energy is found to increase by 1 order of magnitude as compared to the corresponding mixing energy at 150 rpm. In addition, mixing energy is also increased with increasing mixing time.

The torque values and the corresponding mixing energy results have been further analyzed in context to the variation in the electrical conductivity data of PP/MWNTs composites, which is discussed in the subsequent section.

Electrical Characterization

The variation of AC electrical conductivity as a function of frequency for compression-molded PP/MWNTs composite of varying MWNTs concentration is presented in Figure 2. It is observed that the electrical conductivity for pure PP increases with increase in frequency, which is the characteristic of an insulating material. However, PP/MWNTs composite shows a frequency-independent plateau (DC electrical conductivity) followed by a critical frequency (ω_c) beyond which the electrical conductivity increases as a function of frequency. This is consistent with "Johnscher Universal Power Law" for frequency-dependent conductivity of solids.[25] Figure 2 shows the electrical conductivity of PP/MWNTs composite increases gradually along with a gradual shift in ω_c as a function of MWNTs concentration. The corresponding variation in the DC electrical conductivity as a function of MWNTs concentration is plotted in Figure 3 (DC electrical conductivity values are also given in Table II). The electrical percolation threshold is found in between 1.5 and 2 wt % of MWNTs content. A detail discussion on this aspect has been addressed in Ref. [12].

Frequency-dependent electrical conductivity at room temperature for PP/MWNTs composites of 3 wt % MWNTs as a function of melt-mixing temperature is presented in Figure 4(a). Electrical conductivity of PP/MWNTs composites processed at 200 and 220°C exhibit insulating behavior with a value of about 10^{-14} S/cm at 0.1 Hz. PP/MWNTs composites processed at 240°C show a frequency-independent plateau (DC conductivity) up to a critical frequency ($\omega_c = 1.2 \times 10^{-10}$ Hz) above which the conductivity increases with increase in frequency. An abrupt

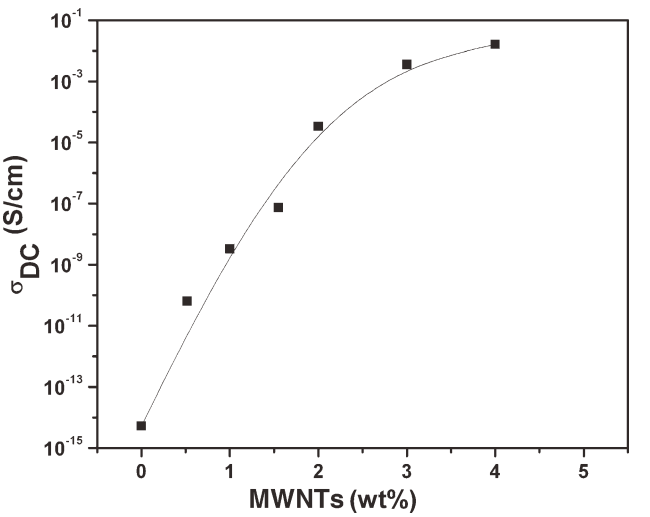

Figure 3. Variation of DC electrical conductivity as a function of MWNTs concentration for compression-molded PP/MWNTs composites.

Table II. DC Electrical Conductivity of Compression Molded PP/MWNTs Composites

Sr. no.	Sample code	σ_{DC} (S/cm)
1	PP	5.3×10^{-15}
2	PP + 0.5 wt % MWNTs	1.0×10^{-10}
3	PP + 1 wt % MWNTs	3.3×10^{-9}
4	PP + 1.5 wt % MWNTs	8.7×10^{-8}
5	PP + 2 wt % MWNTs	3.3×10^{-5}
6	PP + 3 wt % MWNTs	3.5×10^{-3}
7	PP + 4 wt % MWNTs	1.6×10^{-2}

increase in electrical conductivity is observed for PP/MWNTs composites processed at 260°C, wherein the electrical conductivity is independent over a wide range of frequency indicating the formation of percolating network-like structure of MWNTs. It has been reported earlier that the percolation threshold of MWNTs is found between 1.5 and 2 wt % of MWNTs in compression-molded PP/MWNTs composites.[12] Henceforth, injection-molded PP/MWNTs composites of 3 wt % MWNTs in the present context should exhibit a well-defined network-like structure in 3D considering the fact that injection-molded PP/MWNTs composites would exhibit a higher percolation threshold as compared to compression-molded specimen. Considering the variation in electrical conductivity in PP/MWNTs composites with increase in melt-mixing temperature, it is suggested that the formation of percolating network-like structure of MWNTs is facilitated at higher melt-mixing temperature. Moreover, the formation of percolating network-like structure of MWNTs may possibly be associated with the smaller sized aggregates or even individual MWNTs at higher melt-mixing temperature as shear-induced deformation of the polymer chains more easily infiltrate between the nanotubes during melt mixing, which otherwise favors the breakdown the MWNTs aggregates.[27] The highest electrical conductivity ($\sim 10^{-5}$ S/cm) in PP/MWNTs composites corresponds to a mixing energy of $\sim$ 5491 J/cm^3 at a melt-mixing temperature of 260°C. It is also observed that the mixing energy varies from 8886 to 5491 J/cm^3 while increasing the melt-mixing temperature from 200 to 260°C for PP/MWNTs composites. The observed variation in mixing energy with increase in melt-mixing temperature is in agreement with the reported results[8,27–29] in a gross sense. Moreover, the absolute value of mixing energy corresponding to the highest electrical conductivity is much higher in PP/MWNTs composites as compared to PA6/MWNTs and PC/MWNTs composites.[8,27–29] In the current context, it may be argued that MWNTs network-like structure is favored at the highest melt-mixing temperature due to the fact that PP melt could flow into the MWNTs aggregates uniformly at the early stage of melt mixing as compared to the melt mixing at lower temperature in which the PP melt viscosity would be much higher. The adsorption of polymer chains on the MWNTs aggregates uniformly is the key to achieve network-like structure in PP/MWNTs composites. It can also be commented that at lower melt-mixing temperature, MWNTs aggregates should be much finer considering the higher mixing energy during melt mixing. However, nonuniform polymer melt flow (due to higher melt viscosity) into the MWNTs aggregates may lead to a poor distribution of MWNTs in the PP matrix during melt

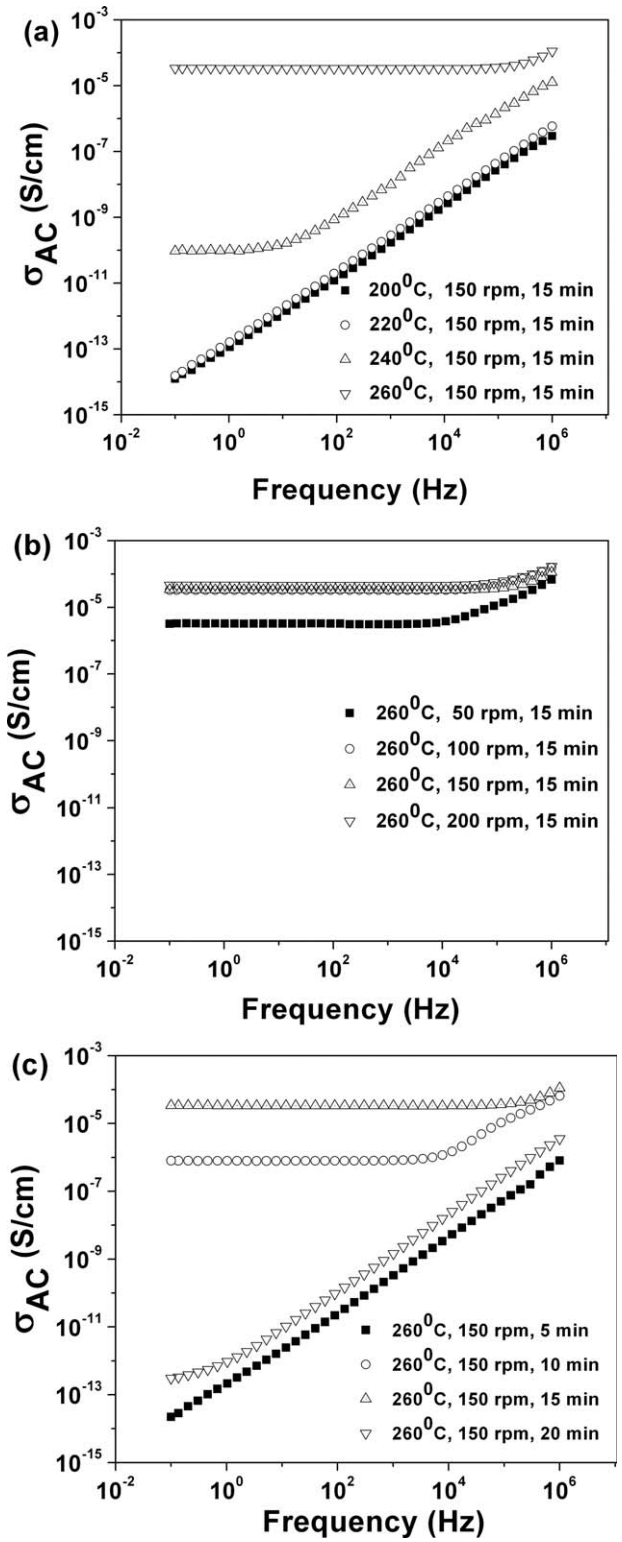

Figure 4. Variation of AC electrical conductivity as a function of (a) mixing temperature, (b) screw speed, and (c) residence time during melt mixing of PP and MWNTs for injection-molded sample.

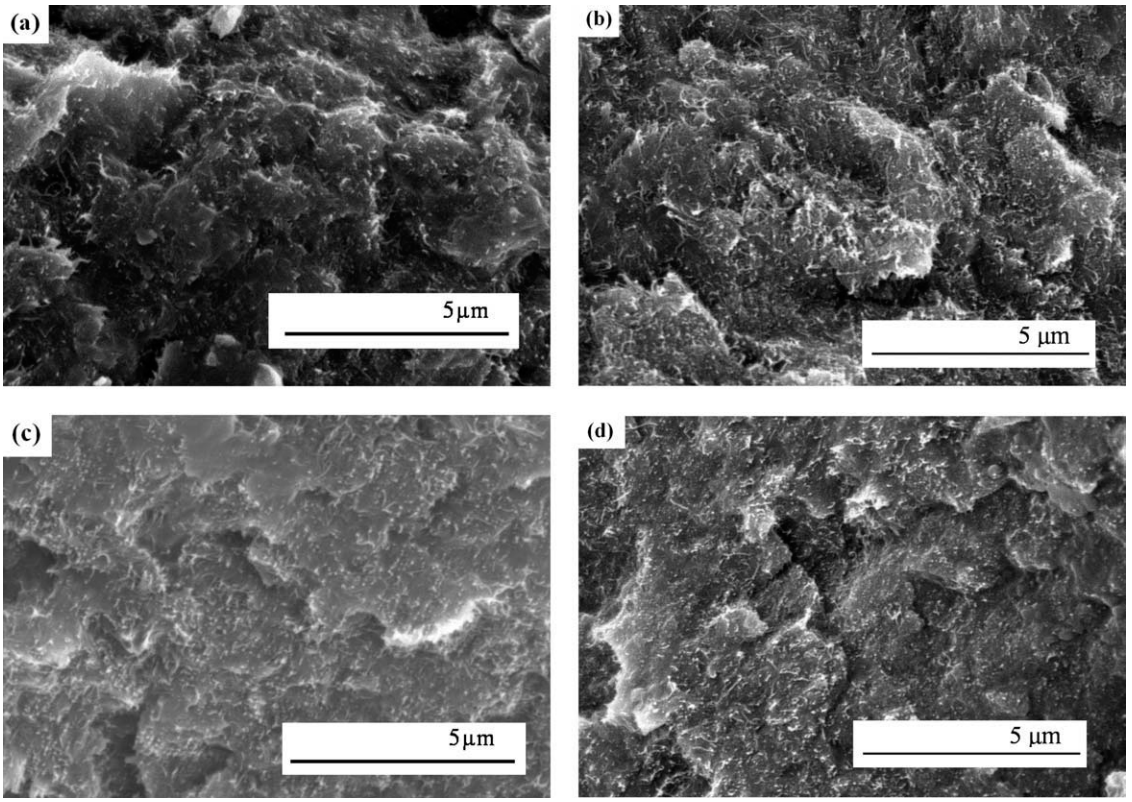

Figure 5. SEM images of cryofractured extruded strands of PP/MWNTs composites: (a) Ti-5, (b) Ti-15, (c) Ti-20, and (d) R-100.

mixing. Moreover, MWNTs breakage cannot be ruled out. These two factors may dominate the network-like structure of MWNTs in the PP matrix at higher mixing energy.

Frequency-dependent electrical conductivity at room temperature for PP/MWNTs composites (3 wt % MWNTs) as a function of screw speed during melt mixing is presented in Figure 4(b). Electrical conductivity is independent over a wide range of frequency for PP/MWNTs composites processed at 50 rpm indicating the formation of percolating network-like structure of MWNTs. PP/MWNTs composites (3 wt % MWNTs) processed higher than 50 rpm (*viz.*, 100–200 rpm) exhibit a marginal increase in electrical conductivity nearly by 1 order of magnitude in various other combinations. Electrical conductivity data also suggest that variation in melt-mixing temperature is a more dominant factor as compared to the varying screw speed during melt-mixing in achieving finer percolating network-like structure of MWNTs in PP matrix. In contrast, the highest electrical conductivity of PP/MWNTs composites processed at 200 rpm corresponds to $\sim$ 8440 J/cm^3 of mixing energy. As discussed, a marginal variation in electrical conductivity is observed as a function of increasing screw speed (50–200 rpm), which corresponds to a wide variation in mixing energy (832–8440 J/cm^3). The variation in mixing energy in this case cannot be explained on the basis of remaining aggregates size of MWNTs in PP/MWNTs composites. The variation in electrical conductivity in these composites cannot be explained by mixing energy concept. A more detailed morphological investigation is necessary to address this issue.

Frequency-dependent electrical conductivity at room temperature for PP/MWNTs composites as a function of melt-mixing time is shown in Figure 4(c). PP/MWNTs composites processed for 5 min show insulating behavior with a value about 10^{-14} S/cm at 0.1 Hz. An abrupt increase in electrical conductivity (about 8 orders of magnitude) is observed for PP/MWNTs processed for 10 min, wherein the electrical conductivity is independent over a wide range of frequency indicating the formation of percolating "network-like structure" of MWNTs. With further increase in mixing time (15 min), composites exhibit marginally higher electrical conductivity as compared to the electrical conductivity of the composites processed for 10 min of mixing time. Composite exhibits sudden drop in electrical conductivity showing insulating behavior with further increase in mixing time of 20 min. This observation suggests that a critical mixing time is required to debundle the MWNTs aggregates. However, excessive shearing action for longer time duration may lead to breakage/shortening of MWNTs as indicated by the destruction of network-like structure of MWNTs in PP matrix, which may need TEM verification. It may be argued that mixing energy concept could not explain effectively the variation in the electrical conductivity in PP/MWNTs composites. The network-like structure of MWNTs may be influenced by the various events taking place during melt mixing: (a) the adsorption/infiltration of polymer chains on the MWNTs surface (a higher melt-mixing temperature and a polar polymer leads to more uniform adsorption of polymer chains into the MWNTs aggregates), (b) shear-induced unentanglement of MWNTs aggregates leading to a finer network, and (c) shear induced MWNTs

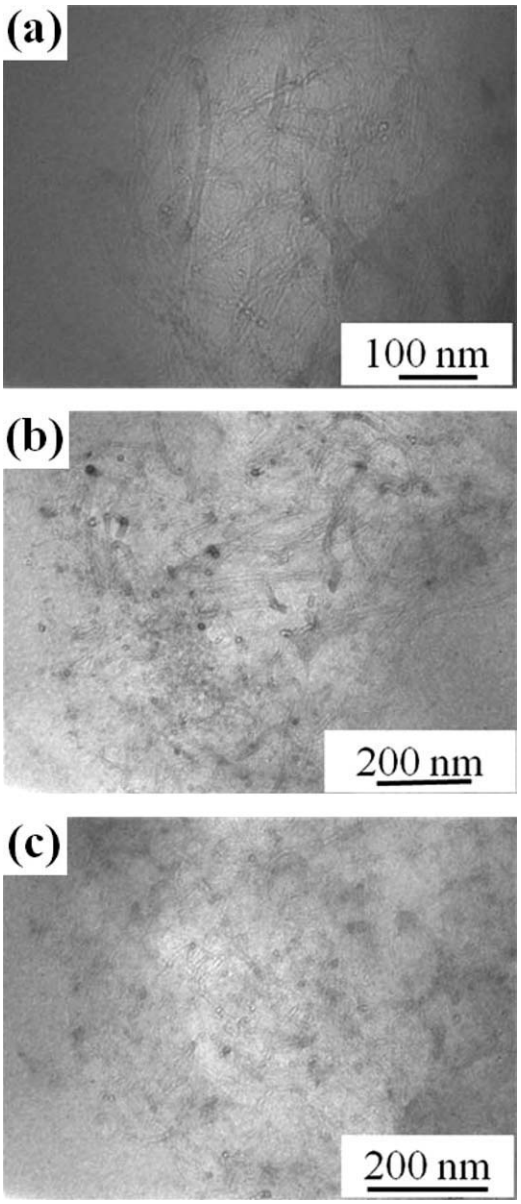

Figure 6. TEM images of ultramicrotomed core section of injection-molded PP/MWNTs composites: (a) T-200, (b) Ti-5, and (c) T-240.

attrition and also polymer chain degradation for prolonged mixing time/higher shearing action. It is also to be mentioned that the composites prepared in the chaotic mixer have been shown to exhibit lower electrical percolation threshold and have been attributed to much less attrition of the high aspect ratio conducting filler during chaotic mixing as compared to internal mixer and also due to a difference in flow mechanism.[30,31]

Morphological Characterization

Scanning Electron Microscopy. Figure 5 exhibits SEM images of representative compositions of cryofractured PP/MWNTs composites of 3 wt % MWNTs processed by varying melt-mixing parameters. It is observed from these micrographs that MWNTs are dispersed uniformly in the PP matrix irrespective of their mixing protocol. However, the state of dispersion of MWNTs cannot be differentiated well in the respective SEM images to understand the effect of melt-mixing parameters on the state of dispersion of MWNTs. It is also noticed that interconnected MWNTs along with well-separated MWNTs exist for

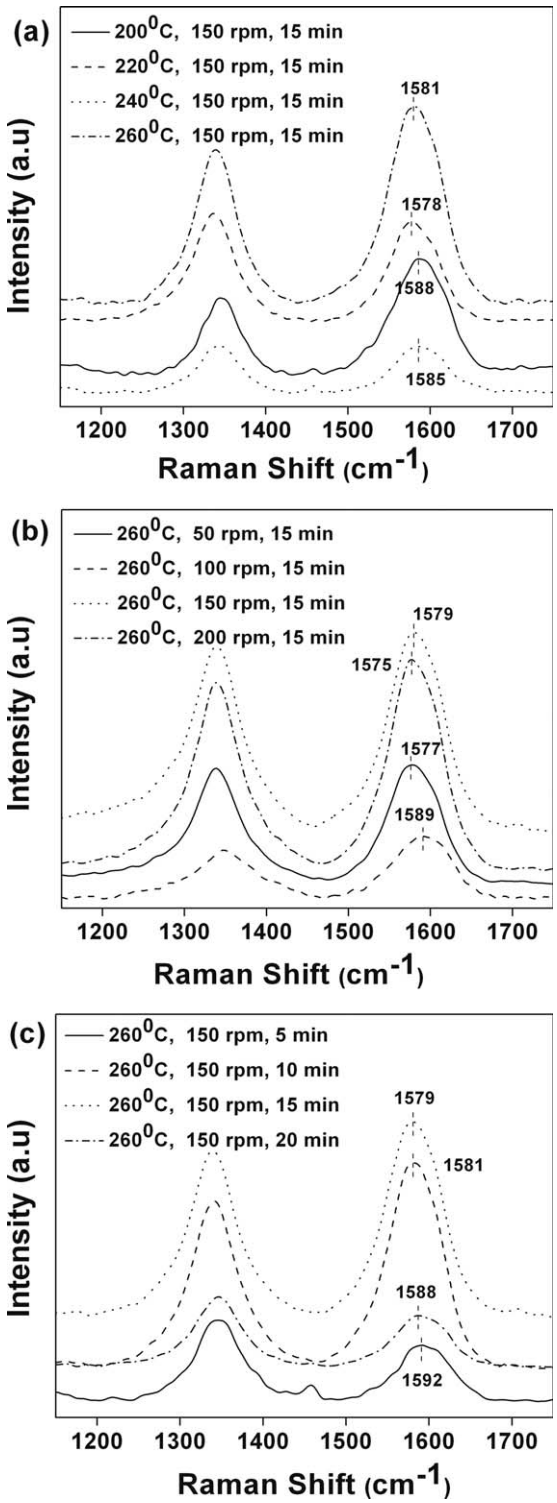

Figure 7. Raman spectra of injection-molded PP/MWNTs composites of skin region of varying melt-mixing parameters (a) temperature, (b) screw speed, and (c) residence time.

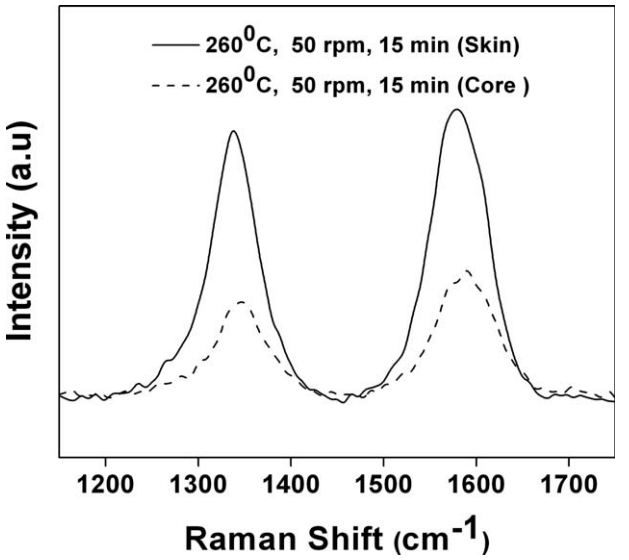

Figure 8. Raman spectra of a representative PP/MWNTs composite of both skin and core regions.

a given composition [Figure 5(a,c,d)]. Figure 6(b) shows the development of a "percolating network" of MWNTs in the PP matrix. It is to be mentioned that the variation in MWNTs percolated structure as a function of melt-mixing parameters cannot be commented unequivocally through SEM observations. In this context TEM investigations have been performed for representative PP/MWNTs compositions of varying melt-mixing parameters. In contrary, TEM investigations [Figure 6(a–c)] suggest the formation of MWNTs cluster in the PP matrix. "Cluster–cluster" interconnectivity is not seen in these compositions (even at lower magnification, corresponding figures are not shown here), which is also expected as these compositions do not show electrically conducting. A detailed TEM investigation is addressed for future investigation for various compositions of PP/MWNTs composites of the skin and the core region of the injection-molded sample to understand the variation of network-like structure of MWNTs as a function of melt-mixing parameters.

Raman Spectroscopy. One of the most viable routes of fabricating-molded articles industrially is the injection molding. However, an important issue needs to be addressed in connection with the state of dispersion of MWNTs in injection-molded specimen. The complexity primarily arises because the composites undergo inhomogeneous shear flow within a short span of time during injection molding.[32,33] High-pressure-driven melt flow significantly affects the morphology (orientation and distribution of the MWNTs and polymer chains), which in turn affects significantly the bulk electrical conductivity of the injection-molded specimen. If the melt is cooled down rapidly in a short time, the oriented polymer chains are frozen. The differential cooling between the surface and the core of the injection-molded sample leads to a "skin–core" type of morphology.[34] In the case of conductive filler particles of high aspect ratio, such as MWNTs, orientation leads to a difficulty in random network-like structure formation involving skin as well as the core of the injection-molded sample, thus, leads to a shift in the percolation threshold toward higher filler contents.[13,14] In this context, TEM investigations showed oriented MWNTs in the skin region of the PC/MWNTs composites, and the core region represents random MWNTs network.[35]

Raman spectra of PP/MWNTs composites of 3 wt % MWNTs processed as a function of melt-mixing parameters (screw speed, mixing time, and temperature) are depicted in Figure 7(a–c). The shift in *G*-band frequencies can serve as a proof of interaction between MWNTs and the polymer matrix. Raman spectra of PP/MWNTs composites indicate significant change in the *G*-band when compared with the corresponding spectrum of MWNTs [Figure 7(a–c)]. The observed shifts manifest the existence of interaction between MWNTs and PP, which is due to the hydrostatic pressure exerted by the PP on MWNTs as reported earlier.[36]

A general observation can be made based on the ratio of intensity of *G*-band to *D*-band (I_G/I_D ratio) of the skin and the core regions of the composite samples with varying melt-mixing parameters. It is known that I_G/I_D ratio of MWNTs indicates the extent of ordered structure associated with MWNTs.[37] This parameter (I_G/I_D ratio) also indicates the quality of MWNTs dispersion in terms of cluster size of MWNTs either in suspension or in the composites.[38] It is important to note that PP/MWNTs composite of 3 wt % MWNTs exhibit a higher value of I_G/I_D of skin as well as of core regions as compared to pure MWNTs (0.87) irrespective of melt-mixing conditions. This indicates that aggregates size of MWNTs is decreased in the composites as compared to pure MWNTs, which is due to the dispersion of MWNTs into smaller aggregates in the PP matrix. Figure 8 compares the Raman spectra for injection-molded samples of skin and core section of PP/MWNTs composites of 3 wt % MWNTs processed at 260°C, 50 rpm, and 15 min. Furthermore, skin region always exhibits higher I_G/I_D value as compared to the corresponding I_G/I_D value of the core region of the same sample (processed under same mixing conditions) irrespective of the melt-mixing parameters (Table III). The higher value of I_G/I_D ratio of MWNTs in the skin region may presumably be related to higher orientation of MWNTs in the skin region. A similar observation can be found in PC/MWNTs composite fiber with increased take-up speed during melt spinning and also in melt spun PP/a-MWNTs (amine functionalized MWNTs) composite fiber as a function of increased draw ratio during postdrawing, which also exhibit higher I_G/I_D ratio as compared to melt-mixed composites.[39,40]

Table III. I_G/I_D Ratio of Skin and Core Region of Injection Molded PP/MWNTs Composites of 3 wt % MWNTs and the Corresponding DC Electrical Conductivity of the Composites

Sr. no.	Sample code	$(I_G/I_D)_{skin}$	$(I_G/I_D)_{core}$	σ_{DC} (S/cm)
1	T-200	1.02	0.96	1.47×10^{-14}
2	T-260	0.99	0.92	3.40×10^{-5}
5	R-50	1.07	0.91	3.16×10^{-6}
6	R-150	0.99	0.92	3.40×10^{-5}
7	R-200	0.99	0.94	4.60×10^{-5}
8	Ti-10	1.01	0.98	7.98×10^{-7}
9	Ti-15	0.99	0.92	3.40×10^{-5}

Furthermore, electrical conductivity of these composites are discussed in connection with I_G/I_D value of the corresponding composite samples of skin and the core regions to understand the effect of varying melt-mixing parameters on the network-like structure of MWNTs in the PP matrix. It is expected that the variation in melt-mixing parameters leads to a change in the aggregates size of MWNTs due to a difference in the extent of infiltration/adsorption of the PP chains in the MWNTs aggregates, which manifests in corresponding variation in I_G/I_D values of the core region (and also in the skin region) of the composites. Core region of the injection-molded composite resembles a similar morphology in terms of random network-like structure formation of MWNTs in the corresponding melt-mixed composites (extrudates). On the other hand, the orientation of MWNTs is a more dominant feature that is reflected in the I_G/I_D value (which higher than core) of the skin region of the composites. During injection molding, oriented skin layer is also observed in PP.[34] Furthermore, during injection molding, orientation of MWNTs in the skin region would be much easier with smaller cluster size of MWNTs in PP/MWNTs composites. In short, higher I_G/I_D values in both the skin as well as core section represent a finer dispersion of MWNTs aggregates; the MWNTs network is more random in nature in the core section, whereas MWNTs network in the skin section is oriented in the flow direction in the injection-molded PP/MWNTs composites. Thus, the difference in I_G/I_D values between the skin and that of the core regions of the composites indicates a varying extent of the network-like structure of MWNTs in the respective composites (Table III). It was expected that composite sample would show higher electrical conductivity wherein the difference between I_G/I_D value of the skin and the core region would be minimum. Although this hypothesis was in agreement with the electrical conductivity results of few samples, a more detail Raman mapping is necessary to validate this hypothesis.

SUMMARY AND CONCLUSION

Melt-mixed PP/MWNTs composites were prepared by varying melt-mixing parameters to assess the variation in network-like structure of MWNTs. This has been achieved by varying melt-mixing temperature, residence time, and screw speed during melt mixing in a conical twin-screw microcompounder.

Melt-mixing temperature has been found to be the most dominant factor in the formation of network-like structure of MWNTs in PP matrix at a fixed screw speed and at a fixed residence time. A higher mixing temperature had a dramatic effect in increasing the electrical conductivity possibly due to a better adsorption of polymer chains into the MWNTs aggregates. Mixing energy concept could not rationalize the variation in electrical conductivity of the injection-molded PP/MWNTs composites, which were prepared by varying melt-mixing parameters.

It was also observed that the I_G/I_D ratio in the skin region was significantly higher than the core region indicating preferential alignment of MWNTs in the skin region during the injection molding step. Morphological observation showed MWNTs cluster as well as individual MWNTs in the PP phase in various PP/MWNTs composites; however, SEM and TEM investigations could not differentiate the MWNTs network in the various compositions of PP/MWNTs composites.

Overall, it can be concluded that electrical conductivity measurements could detect the formation of network-like structure of MWNTs in PP/MWNTs composites, which was influenced by the varying melt-mixing parameters. Because of the anisotropy in the injection-molded PP/MWNTs composites, Raman spectroscopic analysis could provide an insight into the variation of network-like structure of MWNTs.

One of the authors (A. R. B.) would like to acknowledge the Director, DMSRDE Kanpur, India for the financial support for the projects 10DRDO10 and 10DRDO14. The authors duly acknowledge Microcompounder Central Facility at IIT Bombay, CRNTS, IIT Bombay for Raman spectroscopic characterization and also to Amrita V. Poyekar (Research Scholar, IITB-Monash Research Academy) for performing TEM investigations.

REFERENCES

1. Iijima, S. *Nature* **1991,** *354*, 56.
2. Jin, Z.; Pramoda, K. P.; Xu, G.; Goh, S. H. *Chem. Phys. Lett.* **2001,** *337*, 43.
3. Schadler, L. S.; Giannaris, S. C.; Ajayan, P. M. *Appl. Phys. Lett.* **1998,** *73*, 3842.
4. Sandler, J. K. W.; Kirk, J. E.; Kinloch, I. A.; Shaffer, M. S. P.; Windle, A. H. *Polymer* **2003,** *44*, 5893.
5. Wang, M.; Kang, Q.; Pan, N. *Appl. Therm. Eng.* **2009,** *29*, 418.
6. Wang, M.; Meng, F.; Pan, N. *J. Appl. Phys.* **2007,** *102*, 033514.
7. Pötschke, P.; Bhattacharyya, A. R.; Janke, A. *Eur. Polym. J.* **2004,** *40*, 137.
8. Krause, B.; Pötschke, P.; Häußler, L. *Compos. Sci. Technol.* **2009,** *69*, 1505.
9. Kodgire, P. V.; Bhattacharyya, A. R.; Bose, S.; Gupta, N.; Kulkarni, A. R.; Misra, A. *Chem. Phys. Lett.* **2006,** *432*, 480.
10. Bose, S.; Bhattacharyya, A. R.; Kulkarni, A. R.; Pötschke, P. *Compos. Sci. Technol.* **2009,** *69*, 365.
11. Khare, R. A.; Bhattacharyya, A. R.; Kulkarni, A. *J. Appl. Polym. Sci.* **2011,** *392*, 28.
12. Tambe, P.B.; Bhattacharyya, A. R.; Kamath, S.; Kulkarni, A. R.; Sreekumar, T.V.; Mukhopadhyay, K.; Sinha, M. K.; Srivastav, A.; Bhasker Rao, K. U. In Carbon Nanotube Based Nanocomposites: Recent Development; Kar, K. K.; Hodzic, A., Eds.; Research Publishing Services: Singapore, **2011**; p 297–314.
13. Bose, S.; Bhattacharyya, A. R.; Kodgire, P. V.; Kulkarni, A. R.; Misra, A. *J. Nanosci. Nanotechnol.* **2008,** *8*, 1867.
14. Villmow, T.; Pegel, S.; Pötschke, P.; Wagenknecht, U. *Compos. Sci. Technol.* **2008,** *68*, 777.
15. Kharchenko, S. B.; Douglas, J. F.; Obrzut, J.; Grulke, E. A.; Migler, K. B. *Nat. Mater.* **2004,** *3*, 564.
16. Seo, M. K.; Park, S. J. *Chem. Phys. Lett.* **2004,** *395*, 44.
17. Alig, I.; Lellinger, D.; Dudkin, S. M.; Pötschke, P. *Polymer* **2007,** *48*, 1020.

18. Mičušík, M.; Omastová, M.; Krupa, I.; Prokeš, J.; Pissis, P.; Logakis, E.; Pandis, Ch.; Pötschke, P.; Pionteck, J. *J. Appl. Polym. Sci.* **2009,** *113*, 2536.
19. Logakis, E.; Pandis, Ch.; Kyritsis, A.; Pissis, P.; Omastová, M.; Pionteck, J. *Chem. Phys. Lett.* **2010,** *498*, 125.
20. Logakis, E.; Pollatos, E.; Pandis, Ch.; Peoglos, V.; Zuburtikudis, I.; Delides, C. G.; Vatalis, A.; Gjoka, M.; Syskakis, E.; Viras, K.; Pissis, P. *Compos. Sci. Technol.* **2010,** *70*, 328.
21. Radhakrishnan, V. K.; Davis, E. W.; Davis, V. A. *Polym. Eng. Sci.* **2010,** *50*, 1831.
22. Wu, D.; Sun, Y.; Zhang, M. *J. Appl. Polym. Sci.* **2009,** *47*, 608.
23. Socher, R.; Krause, B.; Boldt, R.; Hermasch, S.; Wursche, R.; Pötschke, P. *Compos. Sci. Technol.* **2011,** *71*, 306.
24. Villmow, T.; Pötschke, P.; Pegel, S.; Häussler, L.; Kretzschmar, B. *Polymer* **2008,** *49*, 3500.
25. Jonscher, A. K. *Nature* **1977,** *267*, 673.
26. Baudouin, A.-C.; Auhl, D.; Tao, F. F.; Devaux, J.; Bailly, C. *Polymer* **2011,** *52*, 149.
27. Kasaliwal, G.; Göldel, A.; Pötschke, P. *J. Appl. Polym. Sci.* **2009,** *112*, 3494.
28. Kasaliwal, G. R.; Pegel, S.; Göldel, A.; Pötschke, P.; Heinrich, G. *Polymer* **2010,** *51*, 2708.
29. Kasaliwal, G. R.; Göldel, A.; Pötschke, P.; Heinrich, G. *Polymer* **2011,** *52*, 1027.
30. Gunes, I. S.; Jimenez, G. A.; Jana, S. C. *Carbon* **2009,** *47*, 981.
31. Jimenez, G. A.; Jana, S. C. *Carbon* **2007,** *45*, 2079.
32. Weber, M.; Kamal, M. R. *Polym. Compos.* **1997,** *18*, 711.
33. Wang, M.; Pan, N. *Mat. Sci. Eng. R Rep.* **2008,** *63*, 1.
34. Kantz, M. R.; Newman, H. D.; Stigale, F. H. *J. Appl. Polym. Sci.* **1972,** *16*, 1249.
35. Villmow, T.; Pegel, S.; Pötschke, P.; Wagenknecht, U. *Compos. Sci. Technol.* **2008,** *68*, 777.
36. Liu, L.; Barber, A. H.; Nuriel, S.; Wagner, H. D. *Adv. Funct. Mater.* **2005,** *15*, 975.
37. Strano, M. S.; Moore, V. C.; Miller, M. K.; Allen, M.; J.; Haroz, E. H.; Kittrell, C.; Hauge, R. H.; Smalley, R. E. *J. Nanosci. Nanotechnol.* **2003,** *3*, 81.
38. Khare, R. A.; Bhattacharyya, A. R.; Panwar, A. S.; Bose, S.; Kulkarni, A. R. *Polym. Eng. Sci.* **2011,** *51*, 1891.
39. Pötschke, P.; Brünig, H.; Janke, A.; Fischer, D.; Jehnichen, D. *Polymer* **2005,** *46*, 10355.
40. Tambe, P. B.; Bhattacharyya, A. R.; Kamath, S. S.; Kulkarni, A. R.; Sreekumar, T. V.; Srivastav, A.; Bhasker Rao, K. U.; Liu, Y.; Kumar, S. *Polym. Eng. Sci.* **2012.** DOI: 10.1002/pen.22186.